Mirrorless Optical Parametric Oscillations in Negative-Index Microstructures

A. K. Popov[1], S. A. Myslivets[2], and V. M. Shalaev[3]

[1] *University of Wisconsin-Stevens Point, Stevens Point, WI 54481, USA*
[2] *Institute of Physics of Siberian Division of Russian Academy of Sciences*
Krasnoyarsk 660036, Russian Federation
[3] *Birk Nanotechnology Center and Purdue University, West Lafayette, IN 47907, USA*
e-mail: apopov@uwsp.edu

ABSTRACT

The unique properties of resonant four-wave mixing of backward waves in negative-index materials are investigated. The possibility of realizing miniature mirrorless optical parametric oscillators is shown and their properties are numerically simulated.

Keywords: negative refraction index, metamaterials, compensating losses, backward-wave mirrorless optical parametric micro oscillators, quantum control.

1. INTRODUCTION

Extraordinary properties of mirrorless three-wave mixing backward-wave optical parametric oscillator (OPO) have been predicted in [1-3] and recently demonstrated for the first time [4, 5]. Phase-matching of counter-propagating waves presents a formidable problem and deemed possible in ordinary nonlinear-optical crystals only for frequency quasi-degenerate case. Then one of the coupled waves appears in the far-infrared range. Usually, crystals strongly absorb such radiation. Recent breakthrough has been achieved in submicrometer periodically poled nonlinear-optical crystal which became possible due to the advent of the nanotechnology. However, phase matching of backward waves is inherent to negative-index materials (NIMs). Extraordinary, distributed-feedback, properties of optical parametric coupling and the possibility of the mirrorless OPO (MOPO) in NIMs were predicted in [6-8]. Herewith, we further explore the features of the signal amplification and the properties of micro MOPO followed by the generation of the entangled counter-propagating left-handed signal and right-handed idler photons in NIMs. Two different options are investigated. One is the backward-wave MOPO utilizing intrinsic quadratic nonlinearity of the NIM. Another option is four-wave mixing MOPO based on separately engineered negative refraction index and strong cubic nonlinearity. The latter becomes possible through resonant nonlinear impurities embedded in the NIM. It is shown that the properties of the backward-wave MOPO in the doped NIMs can be tailored by the means of quantum control.

2. MIRRORLESS BACKWARD-WAVE PARAMETRIC MICRO OSCILLATOR

First, we shall illustrate the possibility and extraordinary properties of MOPO based on the intrinsic quadratic nonlinearity of the NIMs [9]. Here, the coupling is off-resonant and linear and nonlinear optical parameters of NIMs do not depend on the intensity of the fundamental (control) radiation.

2.1 Mirrorless optical parametric oscillations in the $\chi^{(2)}$ - NIM

We assume that the wave at ω_1 falls in a negative refraction index domain (NRID), $n(\omega_1) < 0$, and travels with its wave vector k_1 directed along the z-axis [Fig. 1, (a)]. Then its energy-flow S_1 is directed against the z-axis. We also assume that the sample is illuminated by a higher-frequency wave also travelling along the axis z. The frequency of this radiation ω_3, falls in a positive refraction index domain (PRID). The two coupled waves with co-directed wave vectors k_3 and k_1 create a difference-frequency generated (DFG) idler at $\omega_2 = \omega_3 - \omega_1$, which is in a PRID. The idle wave contributes back into the wave at ω_1 through the three-wave coupling and thus enables compensation of losses and amplification (OPA) at ω_1 by converting the energy of the pump field at ω_3. Strong absorption is fundamentally inherent to NIMs and presents a severe obstacle towards numerous breakthrough applications of these revolutionary electromagnetic materials. Thus, the process under consideration involves a three-wave mixing with all wave vectors directed along z. Note that the energy flow of the signal wave, S_1, is directed against z, i.e., it is directed against the energy flows of the two other waves, S_2 and S_3. Such a coupling scheme is in strict contrast with the conventional phase-matching scheme for OPA [Fig. 1, (b)]. The Manley-Rowe relations, which follow from the Maxwell's equations assuming absorption indices $\alpha_1 = \alpha_2 = 0$, have the form:

$$d[(S_{1z}/\hbar\omega_1) - (S_{2z}/\hbar\omega_2)]/dz = 0; \text{ or } d[(\mu_1/\varepsilon_1)^{\frac{1}{2}}(h_1^2/\omega_1) + (\mu_2/\varepsilon_2)^{\frac{1}{2}}(h_2^2/\omega_2)]dz = 0. \tag{1}$$

Here, $h_{1,2}$ are amplitudes of the magnetic components of waves. Equation (1) describes the creation of pairs of entangled counter-propagating photons $\hbar\omega_1$ and $\hbar\omega_2$; it takes into account the opposite signs of the corresponding derivatives with respect to z. The equation predicts that the sum of the terms proportional to the squared amplitudes of the signal and idler remains constant through the sample, which is in strict contrast with the

requirement that the difference of such terms is constant in the case of a PIM. Consequently, the equations for slowly varying amplitudes reveal unusual spatial properties for the three-wave mixing process inside the NIM [c.f., Fig. 1, (c) and (d)], which depends on the product gL and on phase mismatch Δk [Fig. 1, (c), (e), (f)]. Here, g is the factor proportional to the product of squared nonlinear susceptibility and the intensity of the pump field. A strong resonance dependence of the output intensity of the left-handed wave on the factor gL [Fig. 1, (e) and (f)] indicates that unless the pump intensity and the phase matching are appropriately optimized, the maximum of the amplitude of the left-handed wave may occur inside rather than on the output edge of the slab [Fig. 1, (c)]. The OPA can not only fully compensate for absorption but even turn into oscillations when the intensity of the control field reaches values given by a periodic set of increasing numbers [Fig. 1, (e) and (f)]. Amplification in the maxima in Fig. 1, (e) and (f) may reach many orders of magnitude which indicates mirrorless oscillations. Most explicitly, the striking difference between the outlined nonlinear-optical propagation properties is seen in the case when $\alpha_{1,2}$ and $\Delta k \rightarrow 0$. Then, $\eta_{1a} \rightarrow e^{2gz}$ for the ordinary PIMs and $\eta_{1a} \rightarrow |\cos(gz)/\cos(gL)|^2$ for NIMs. Therefore, output signal (at z=0) $\eta_{1a} \rightarrow \infty$ at $gL \rightarrow (j+1)\pi/2$.
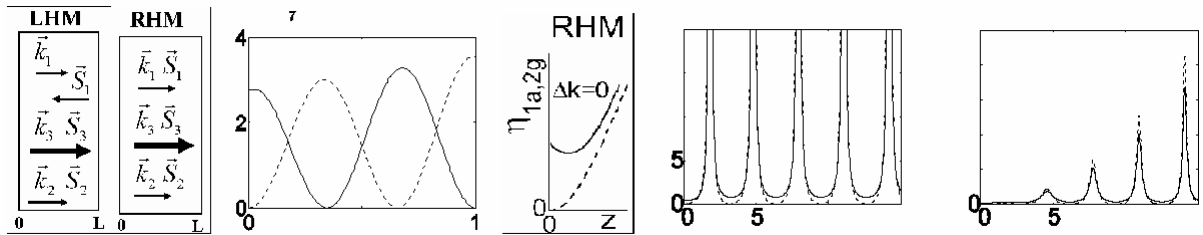

Figure1. The difference between the nonlinear propagation and OPA processes, quadratic nonlinearity [$\chi^{(2)}$], in the left-handed (NIMs) and in the ordinary, positive-index (PIMs), materials. (a) and (b) – phase matching schemes, (c) and (d) – a typical difference in the signal (the solid line) and the idler (the dashed line) spatial intensity distributions. (e)-(f) – output amplification, η_{1a} (the solid line), and the ratio of the intensities of the generated idler and input signal, η_{2g} (the dashed line), for the backward wave at z=0. (e) – phase mismatch $\Delta kL=0$. (f) – $\Delta kL=\pi$. (c), (e) and (f) – absorption $\alpha_1 L=1$, $\alpha_2 L=1/2$.

Hence, the important advantage of the backward OPA, and MOPO in NIMs presented here is the distributed feedback, which is inherent to such scheme and enables oscillations without a cavity. In NIMs, each spatial point serves as a source for the generated wave in the reflected direction, whereas the phase velocities of all the three coupled waves are co-directed. For a more detailed consideration see ref. [6, 7].

2.2 Mirrorless optical parametric oscillations in doped resonant $\chi^{(3)}$ – NIM

The basic idea of the proposed approach is as follows. A slab of NIM is doped by four-level nonlinear centers [Fig. 2, (a)] so that the signal frequency, ω_4, falls in the NRI domain, whereas all the other frequencies, ω_1, ω_2 and ω_3, are in the positive index domain. Below, we show the possibility to produce transparency and even amplification above the oscillation threshold at ω_4 [$n(\omega_4) < 0$] controlled by two lasers at ω_1 and ω_3 with the phase matching propagation settings as shown in Fig. 2, (b). These fields generate idler at $\omega_2 = \omega_1 + \omega_3 - \omega_4$, which experiences population-inversion or Raman amplification caused by the control fields. This opens additional channel of energy transfer from the control fields to the signal. The amplified idler contributes back to $\omega_4 = \omega_1 + \omega_3 - \omega_2$ through FWM and thus causes strongly enhanced OPA of the signal. However, unlike ordinary off-resonant coupling, many-orders resonance enhancement of the processes under investigation is usually followed by a strong change of the local optical parameters by the control fields. Control fields may cause populations transfer and even inversion, modulation of the probability amplitude, split and quantum-interference modification of the resonance shapes and, therefore, may serve as a tool for harnessing local optical coefficients. Alternatively, such changes can be made minimum, so that major amplification would come directly from energy exchange between the control fields, signal and idler through the FWM processes. Interference of quantum pathways in the vicinity of the resonances may even lead to the fact that the overall process ceases to be seen as the set of the successive one- and multi-photon elementary processes. For details, see [10] and references therein. Figure 2, (c)-(f) depicts a distributed feedback feature of such interaction [Fig. 2, (c)], geometrical resonances corresponding to MOPO [Fig. 2, (c), upper left inset, and Fig. 2, (d)] and quantum control of MOPO [Fig. 2, (e) and (f)].

Following data, which are characteristic for molecules embedded in solids, have been used for numerical simulations: optical resonance HWHM $\Gamma \sim 10^{12}$ s^{-1}, Raman resonance HWHM $\Gamma \sim 10^{10}$ s^{-1}, lifetimes $\sim 10^{-8}$ s. Rabi coupling frequencies, G, and frequency detunings, Ω, for corresponding transitions depicted in Fig. 2(a) are taken as $G_1 = G_3 = 50$ GHz, (P ~ 10 kW through Ø ~ 0.1 mm), $\Omega_1 = \Omega_3 = 2.5\ \Gamma_1$, $y_4 = \Omega_4/\Gamma_1$, y_4 (max) ≈ 1.3. For characteristic resonant absorption cross-sections $\sigma_{ra} \sim 10^{-16}$ cm^2 and the density of the embedded resonant centers N $\sim 10^{19}$ cm^{-3} resonance absorption lengths are about $L_{ra} = \alpha_{ra}^{-1} \sim 10^{-3}$ cm and parameter $(|\gamma_2 * \gamma_4|)^{\frac{1}{2}} \approx 0.2\ L_{ra}^{-1}$.

Here, γ_2 and γ_4 are parameters of nonlinear-optical coupling in the equations for the slowly varying amplitudes of the coupled fields. Then the threshold of mirrorless backward-wave optical parametric generation is reached at the NIM slab thickness about $L/L_{ra} \approx 10$, which corresponds to $L \sim (10 \div 100)$ μm. Estimates show that absolute magnitudes of changes in the NRI introduced by the resonant centers are about $\Delta n < 0.5(\lambda/4\pi L_{ra}) \sim 10^{-2} \div 10^{-3}$ and, hence, can be ignored.
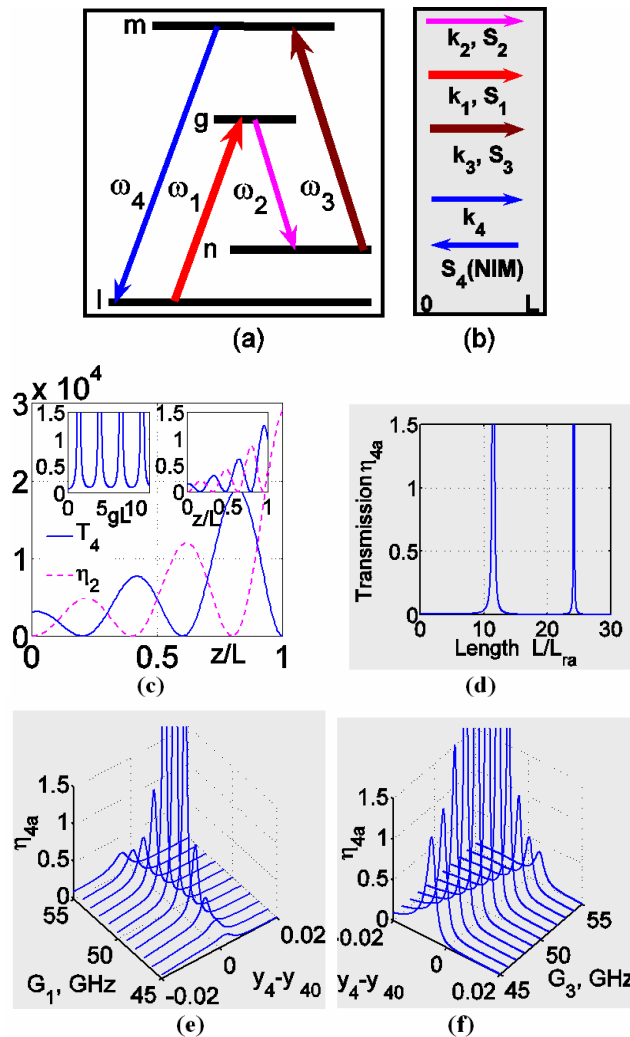

Figure 2 Scheme of quantum controlled FWM interaction (a) and coupling geometry (b). (d)-(f) – transmission resonances and MOPO thresholds. (c) – intensity distribution inside the NIM slab; main plot: solid line – signal, dash line – idler; upper right inset – small variation of the control field; upper left output signal at z = 0. (e) and (f) – dependence of the threshold on the intensity of the control fields and on the signal resonance detunings. Here, ω_4 is frequency of the signal, ω_1 and ω_3 of the control fields, ω_2 of the idler, $n(\omega_4) < 0$.

3. CONCLUSIONS

In conclusion, we propose compensation of losses in strongly absorbing NIMs which is the key problem that determines numerous revolutionary applications of this novel class of electromagnetic materials. Such possibility is explored for OPA based on the off-resonant three-wave nonlinear-optical coupling that utilizes the intrinsic nonlinearity inherent to NIMs. We also propose independent engineering of negative refractive index and strong nonlinear-optical response in the composite metamaterials. The proposed independent engineering of the linear and nonlinear parameters of a NIM is based on the embedded resonant four-level centers which optical response can be tailored through quantum control. Such possibility is proven by the numerical simulations. We have explored the features of off-resonant three-wave mixing and resonant FWM mixing followed by OPA in both types of metamaterials with negative refractive index at the frequency of the signal field and positive index for all other coupled waves. The possibility of creation and the features of mirrorless backward-wave microscopic optical parametric oscillator are investigated for the both, off-resonant $\chi^{(2)}$ and embedded resonant $\chi^{(3)}$, couplings. In addition, for the latter option, we have shown the opportunities of quantum control of the local optical parameters, which employs constructive and destructive quantum interference tailored by two auxiliary driving control fields. The important features of the narrow-band frequency-tuneable transparency windows in the

negative-index frequency domain, cavity-free generation of the entangled counter-propagating photons, and feasibilities of quantum switching in the NIMs have been numerically simulated. The unique features of the proposed photonic devices are revealed, such as strong resonant behaviour in respect of the material thickness and the density of the embedded resonant centers; resonant dependence on the intensity of the control fields, the requirement of the pre-set linear phase-mismatch and the important role of nonparametric amplification of the idler.

ACKNOWLEDGEMENTS

REFERENCES

[1]   S. Harris, Proposed backward wave oscillations in the infrared, *Appl. Phys. Lett.*, vol. 9, pp. 114-117, 1966.

[2]   K. I. Volyak and A. S. Gorshkov, *Radiotekhnika i Elektronika (Radiotechnics and Electronics)*, Moscow, in Russian, v. 18, pp. 2075-2084, 1973.

[3]   A. Yariv, *Quantum Electronics*, 2nd ed. (New York: Wiley, 1975), ch. 18, pp. 465-467.

[4]   J. B. Khurgin, Mirrorless magic, *Nat. Photonics*, vol. 1, no. 8, pp. 446-447, 2007.

[5]   C. Canalias and V. Pasiskevicius, Mirrorless optical parametric oscillator, *Nat. Photonics*, vol. 1, no. 8, pp. 459-462, 2007.

[6]   A. K. Popov and V. M. Shalaev, Negative-index metamaterials: second-harmonic generation, Manley-Rowe relations and parametric amplifications, *Appl. Phys. B* , vol. 84, pp. 131-137, 2006.

[7]   A. K. Popov and V. M. Shalaev, Compensating losses in negative-index metamaterials by optical parametric amplification, *Opt. Lett.*, vol. 31, no. 14, pp. 2169-2171, 2006.

[8]   A. K. Popov, S. A. Myslivets, T. F. George and V. M. Shalaev, Four-wave mixing, quantum control, and compensating losses in doped negative-index photonic metamaterials, *Opt. Lett.*, vol. 32, no. 20, pp.3044-30046, 2007.

[9]   M. W. Klein, M. Wegener, N. Feth and S. Linden, Experiments on second- and third-harmonic generation from magnetic metamaterials, *Opt. Express*, vol. 15, pp. 5238-5247, 2007.

[10] A. K. Popov, S. A. Myslivets and T. F. George, Nonlinear interference effects and all-optical switching in optically-dense inhomogeneously-broadened media, *Phys. Rev. A* , vol. 71, 043811(1-13), 2005.